ELSEVIER

Journal of Alloys and Compounds 330–332 (2002) 841–845

Journal of ALLOYS AND COMPOUNDS

www.elsevier.com/locate/jallcom

Improvement of electrode performances of Mg_2Ni by mechanical alloying

Sang Soo Han, Hee Yong Lee, Nam Hoon Goo, Woon Tae Jeong, Kyung Sub Lee*

Division of Materials Science and Engineering, Hanyang University, 133-791 Seoul, South Korea

Abstract

Nanocrystalline and amorphous Mg_2Ni-based hydrogen storage alloys for Ni–MH batteries had been synthesized by mechanical alloying. The surface modification and Zr addition had also been carried out for improvement of its electrode performance. In comparison with the arc-melted polycrystalline one, the nanocystalline Mg_2Ni phase showed a higher discharge capacity. By increasing milling time from 120 to 160 h, the grain size of Mg_2Ni phase was more refined and the discharge capacity was raised from 180 to 370 mAh g^{-1}. The discharge capacity of the 160-h milled Mg–Ni–Zr amorphous alloys also reached 530 mAh g^{-1}. XPS (X-ray photoelectron spectroscopy) analysis showed that Mg2p spectra were shifted to lower binding energy implying the enhancement of the hydrogen diffusion and charge transfer reaction, and resulted in increasing the discharge capacity in amorphous alloys. To prevent the rapid degradation, the alloy powders were also coated with Ni and graphite by additional ball milling. The Ni and graphite protected the Mg from oxidation, and the coated powders showed a better cyclic stability. After 50 cycles, the degradation of bare electrode was 94% of maximum capacity, but that of coated electrode with Ni and graphite was 45 and 76% of maximum capacity, respectively. © 2002 Elsevier Science B.V. All rights reserved.

Keywords: Nanocrystalline/amorphous; Zr addition; Surface modification

1. Introduction

Mg_2Ni-type metal hydride is the promising material due to the large hydrogen capacity (up to 3.6 wt%), low cost, light weight, and non-toxicity. However, the polycrystalline Mg_2Ni shows a very low electrochemical discharge capacity (less than 10 mAh g^{-1}) [1]. Its capacity has been improved by employing a mechanical alloying [2–4]. In our previous work [5], the nanocrystalline Mg_2Ni phase with grain size less than 50 nm was successfully synthesized by mechanical alloying, and the discharge capacity reached 200 mAh g^{-1} at room temperature. This discharge capacity value is far less than the theoretical discharge capacity of Mg_2Ni phase, 999 mAh g^{-1}. And the cyclic stability of the mechanically alloyed Mg_2Ni phase is so poor that only about 20% of the maximum capacity remains after ten cycles [5]. Although the application of a mechanical alloying process for producing Mg_2Ni alloy looks promising, there still exist the problems of low discharge capacity, poor cycle life, and poor high-rate discharge capability.

In this work, we have selected the synthesis of nanocrystalline/amorphous alloys, the addition of Zr as a third element and the surface modification (mechanical coating) with Ni, graphite elemental powders in order to obtain better electrode performances of Mg_2Ni type alloys. The structural and electrochemical discharge properties have been investigated.

2. Experimental

The elemental powders were mixed at the desired composition. The mixed powders were charged into the Cr–Ni steel vials with the SUS balls of 2/16 inch size. The ball-to-powder ratio was 15:1. The mechanical alloying was performed in argon atmosphere with planetary ball mill (Fritsch. Pulverisette P-5). The milling speed was 100 rpm and duration time was 120 and 160 h. Induction melted polycrystalline Mg_2Ni alloy was obtained from Japan Metals and Chemicals Co. Ltd.

The structural properties of the alloy powders were characterized by X-ray diffraction (Cu Kα, Rigaku D-MAX 3000) and TEM observation. To investigate the changes of binding energy for Mg element on the alloy surface with change of Zr contents, XPS measurements were carried out with SSI 2803-S spectrometer. The source was monochromatic Al Kα radiation (1486.6 eV). The surface of alloy powders was cleaned for 20 s by Ar^+ bombardment with kinetic energy of 4 eV. The etching rate

*Corresponding author.

0925-8388/02/$ – see front matter © 2002 Elsevier Science B.V. All rights reserved.
PII: S0925-8388(01)01654-1

was 100 Å min^{-1}. After cleaning surface, narrow-scan spectra were measured for Mg2p at 55 eV pass energy. The C1s peak at 286 eV was used for internal reference to calibrate the peak position. All electrochemical experiments were tested by the same methods reported in our previous report [5].

To prolong cyclic life of the Mg_2Ni type alloys electrodes, mechanical coatings with Ni and graphite were carried out and the electrode pellets were prepared using these coated powders. A two-step milling process was introduced for coating process. The first step was conducted with 4/16 inch balls, balls to powder ratio of 60:1, for 60 min at 200 rpm. In the first step, only elemental coating powders were charged and milled to make them suitable for coating. In the second step, the pre-milled coating powders and mechanically alloyed powders were charged. The second step was conducted with 2/16 inch balls, ball-to-powder ratio of 100:1 for 70 min at 150 rpm. The electrochemical properties of the coated electrode were compared with the uncoated.

3. Results and discussion

3.1. Structural properties

Fig. 1 shows the XRD patterns of as-milled 2Mg–Ni, 1.8Mg–0.2Zr–Ni and 1.4Mg–0.6Zr–Ni powders. Firstly, in 2Mg–Ni system, after 120 h milling, although the elemental Ni peaks remained, Mg peaks disappeared, and Mg_2Ni phase formed. The elemental Ni peaks did not disappear by further milling. The diffraction patterns of both 120- and 160-h milled powders exhibited the peak broadening which was the characteristics of nanocrystalline material containing many defects. Because peak broadening in 160-h milled powder was wider than that in 120-h milled, it can be considered that the average grain size was smaller in 160-h than in 120-h milled. A large grain boundary area and many defects in the crystal were the typical characteristics of the mechanically alloyed powders [6]. The former may accelerate the diffusion of the hydrogen into the bulk alloy and the latter may act as the hydrogenation sites. It is thought that the nanocrystalline phase with more refined grain has improved hydrogenation characteristics.

Secondly, Zr was added to Mg–Ni powder mixtures for partially substitution for Mg. The composition of mixtures was 1.8Mg–0.2Zr–Ni. The XRD pattern of 120-h milled 1.8Mg–0.2Zr–Ni powders shows a maximum broadening of Mg_2Ni peaks, which indicates the loss of crystallinity and the formation of amorphous structure. According to our previous paper [7], it was reported that the ball-milled 1.8Mg–0.2Zr–Ni powders had the composite like structure made up of amorphous matrix and nanocrystalline precipitates. The precipitates were confirmed to the Mg_2Ni phase in electron diffraction pattern. To prepare the complete

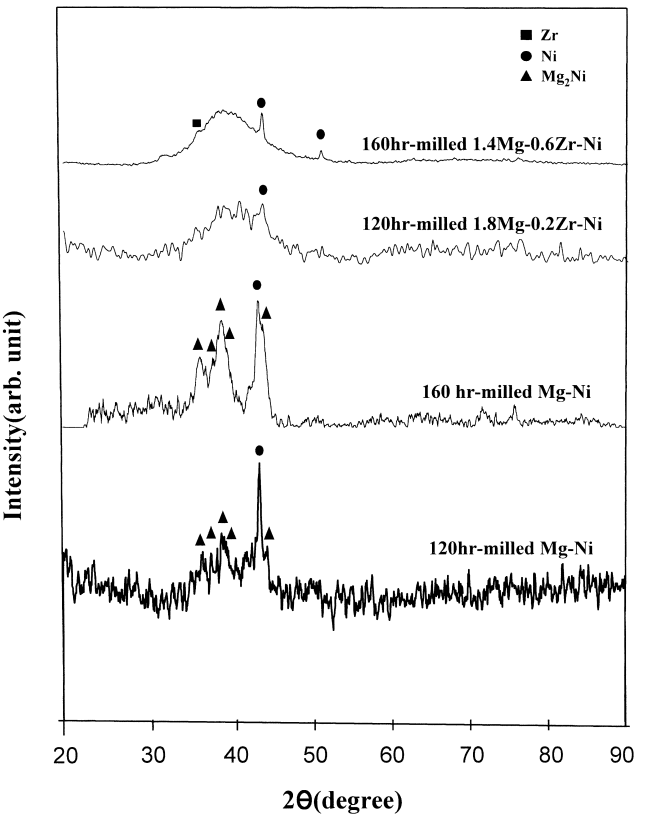

Fig. 1. XRD patterns of Mg_2Ni with milling time and Zr additions.

amorphous phase, the amount of Zr was increased to the composition 1.4Mg–0.6Zr–Ni, and the milling time also increased up to 160 h. Although the elemental Zr, Ni peaks remained, the Mg_2Ni peaks completely disappeared. In the electron diffraction pattern [7], there was no detection of Mg_2Ni ring patterns. The powders consisted of amorphous phase and unreacted Zr, Ni. The Zr addition into Mg_2Ni alloy caused the lattice volume expansion and the amophization of crystalline phase because the atomic radius of Zr (2.16 Å) was larger than that of Mg (1.72 Å) or Ni (1.62 Å).

3.2. XPS analysis of Mg

We had already reported the Mg2p spectra of Mg–Ni alloys with various Zr contents [8]. In comparison with polycrystalline and nanocrystaline Mg_2Ni, the energy band of Mg2p for mechanically alloyed nanocrystalline Mg_2Ni shifted to a lower energy than that of polycrystalline Mg_2Ni. Also with increasing Zr contents, the Mg2p peak shifted further toward the lower energy and the intensity of the peak was relatively increased with respect to that of polycrystalline Mg_2Ni.

From these results, it could be considered that the addition of Zr changed the surface states of these alloys and enhanced hydrogen reactivity at the surface. Also, the

electrons donated from reaction of Zr with Mg were trapped on the alloy surface and trapped electrons changed the electron density and chemical states of both Mg and Ni. These could enhance the charge transfer reaction and hydrogen diffusion ability, which resulted in improving the discharge capacity of Mg_2Ni (Fig. 2) and the high-rate discharge capability [7].

3.3. Electrochemical properties

The electrochemical cycle test data for as-milled 2Mg–Ni, 1.8Mg–0.2Zr–Ni and 1.4Mg–0.6Zr–Ni systems are shown in Fig. 2. The discharge capacity of 120-h milled Mg_2Ni electrode was 170 mAh g^{-1}. It is much more than that of the polycrystalline one reported previously. The formation of nanostructured alloys by MA improved the electrochemical hydrogenation ability of Mg_2Ni electrode at low temperature. In Fig. 2, the 160-h milled Mg_2Ni phase had a larger discharge capacity than the 120-h one. The discharge capacity of 160-h milled Mg_2Ni was 370 mAh g^{-1} at the first cycle with no activation. The increase of milling time made more defects and refined grains, which made the Mg_2Ni phase more active to absorb/desorb hydrogen.

It is also shown that the partial substitution of Zr for Mg increased the discharge capacity of Mg_2Ni. The discharge capacity of 120-h milled 1.8Mg–0.2Zr–Ni powder was 465 mAh g^{-1} at the first cycle. This is related to the composite structure including the amorphous matrix and nanocrystalline Mg_2Ni precipitates. The nanocrystalline precipitates disappeared by further ball-milling and more addition of Zr, and there existed Mg–Ni–Zr ternary amorphous phase and elemental Ni and Zr powder. The discharge capacity of 160-h milled 1.4Mg–0.6Zr–Ni reached the highest capacity of 530 mAh g^{-1}. With the addition of Zr, the increase of discharge capacity resulted from the amorphization and the decrease of binding energy of Mg at the surface. For amorphous metal hydride, the diffusivity and solubility of hydrogen are reported to be larger than those in crystalline phase, since amorphous alloys don't have a long range order but the nearest neighbor or local order [3,9].

The hydriding reaction mechanism of amorphous phase is not clear, and there are some conflicting reports on the hydriding/dehydriding properties of amorphous hydride [3,9,10]. Liu et al. [3] reported that the Mg–Ni amorphous phase synthesized by mechanical alloying had the room temperature electrochemical hydrogen storage ability, and remarkably increased the discharge capacity in comparison with the polycrystalline one. Fig. 3 shows the galvanostatic charge curves of amorphous and nanocrystalline metal hydride. The amorphous phase was 160-h milled 1.4Mg–0.6Zr–Ni powder, and the nanocrystalline was 160-h milled 2Mg–Ni powder. The potential plateau region of amorphous is longer than that of nanocrystalline, indicating that the larger hydrogen solubility of amorphous phase. The increased discharge capacity of amorphous phase is related to larger hydrogen solubility, and enhanced charge transfer reaction and hydrogen diffusion ability. Similar to polycrystalline Mg_2Ni, however, the rapid degradation of nanocrystalline and amorphous alloys was also observed. The reason is also related to the binding properties of each element at the surface.

3.4. Surface modification by mechanical coating

We have previously reported that a rapid degradation in mechanical alloyed Mg_2Ni was because magnesium in Mg_2Ni was easily oxidized in alkaline solution and

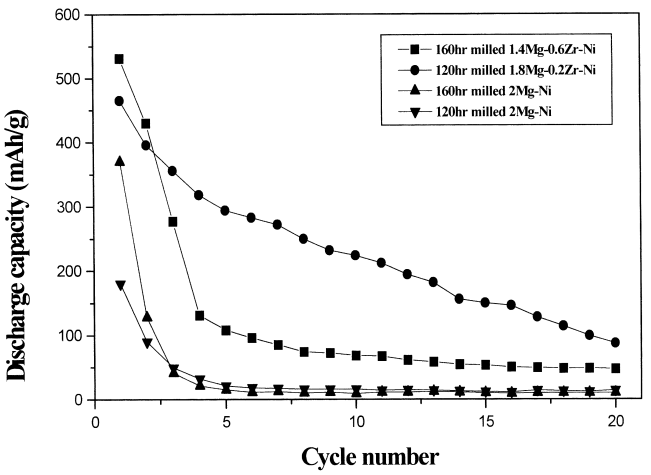

Fig. 2. Cycle test data of nanocrystalline Mg_2Ni alloys and amorphous Mg–Zr–Ni alloys.

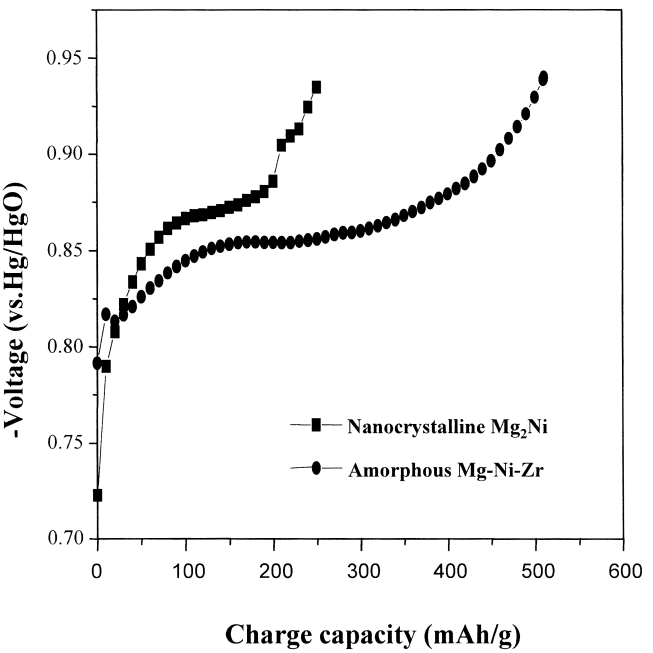

Fig. 3. Galvanostatic charge curves of nanocrystalline and amorphous alloys.

$Mg(OH)_2$ passive film was formed [5]. The surface modification may be very effective to protect the passivation of the alloy surface. The mechanical coating method has been chosen in this study. This mechanical coating has some merits. It dose not require an additional process, or the use of a toxic solution as in the case of chemical coating.

In case of Ni coating [5], the active material and Ni were elongated to form the lamellar-type layers. However, the graphite coating layers were not as dense as Ni coating layers. As shown in Fig. 4, the bright region was Mg_2Ni active material and the dark was graphite powder. Mg_2Ni powders were simply embedded into the graphite layer, which had many micro cracks formed during ball-milling.

The electrodes prepared from the coated powders had better cyclic stability than those from bare ones (Fig. 5). After 50 cycles, the degradation of bare electrode was 94% of maximum capacity, but that of coated electrode with Ni and graphite was 45 and 76% of maximum capacity, respectively. The Ni coating was more effective in protecting the alloy surface than the graphite coating. The graphite coating raised the maximum electrode capacity, but did not greatly improve the cyclic stability. This is caused by the micro cracks existing on the graphite coating layer. The reason that the maximum capacity is higher in

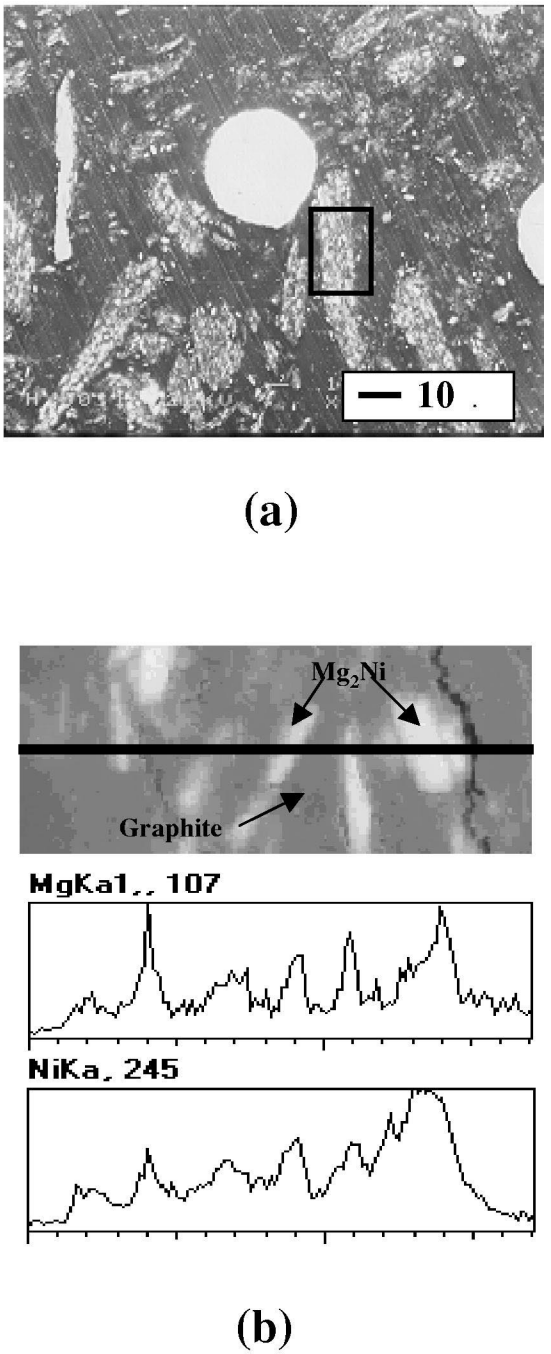

Fig. 4. SEM micrographs and EDX line mapping of the mechanically coated Mg_2Ni powder with the graphite. (a) Cross sectional image of the graphite-coated powder. (b) EDX line-mapping of Mg.

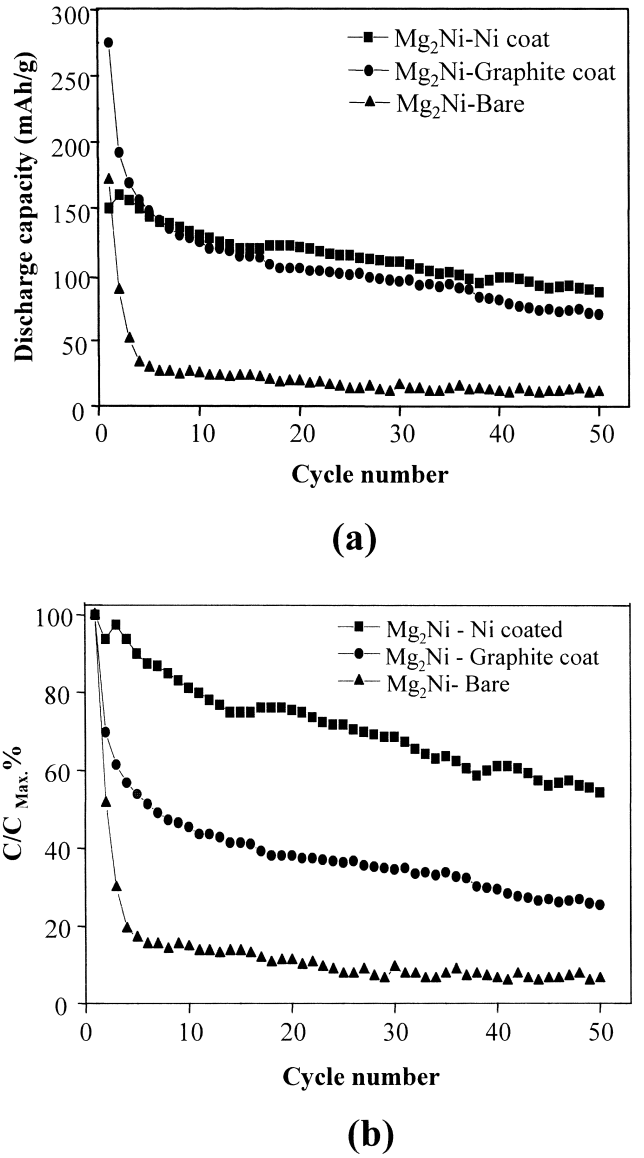

Fig. 5. Cycle test data of the electrode mechanically coated with nickel and graphite. (a) The discharge capacity. (b) The cyclic life.

graphite coating (275 mAh g^{-1}) than in Ni (170 mAh g^{-1}) is because the electrical conductivity of graphite is higher than that of Ni. Compared to that of the uncoated material, the degradation of the coated powders was suppressed by the mechanical coating with nickel and graphite.

The differences of the Ni and graphite coatings were summarized as follows. In the aspect of morphology, the Ni coating had a dense lamellar structure, while the graphite one had many micro-cracks between the graphite and the Mg_2Ni. And in the aspect of electrochemical properties, although the maximum discharge capacity was higher in the case of graphite coating (275 mAh g^{-1}) than that of the Ni one (170 mAh g^{-1}), the cyclic stability was better in the Ni coating than in the graphite one.

4. Conclusion

The nanocrystalline and amorphous Mg_2Ni-based alloys were synthesized successfully by MA. The nanocrystalline Mg_2Ni phase had higher discharge capacity at room temperature than the polycrystalline one. The increase of milling time made the more refined grain structure, which cause the increase of discharge capacity. The Zr additions appreciably enhanced the structural disorder and a ternary amorphous phase of Mg–Ni–Zr was formed. Because of the formation of an amorphous phase induced by Zr addition, the maximum discharge capacity was increased. In XPS analysis, with Zr addition in Mg–Ni alloys, Mg2p spectra shifted to the lower energy state, which implied that the charge transfer reaction and hydrogen diffusion were enhanced, and then the discharge capacity was increased. However, the mechanically alloyed electrode was degraded very rapidly with cycles. The Ni and graphite coating layer protected the Mg from oxidation, and the coated powders showed better cyclic stability than the bare one. The Ni coated powder had a dense lamellar-type morphology, but the graphite coated one had micro-cracks along the active material surface. The Ni coating was more effective in protecting surface from oxidation than the graphite coating.

Acknowledgements

This work was supported by the Brain Korea 21 project.

References

[1] N. Cui, B. Luan, H.J. Zhao, H.K. Lin, S.X. Dou, J. Alloys Comp. 240 (1996) 229.
[2] J.H. Woo, K.S. Lee, J. Electrochem. Soc. 146 (3) (1999) 819.
[3] W. Liu, H. Wu, Y. Lei, Q. Wang, J. Wu, J. Alloys Comp. 252 (1997) 234.
[4] M. Abdellaoui, D. Cracco, A. Percheron-Guegan, J. Alloys Comp. 268 (1998) 233.
[5] N.H. Goo, J.H. Woo, K.S. Lee, J. Alloys Comp. 288 (1999) 286.
[6] C. Suryanarayana, Int. Mater. Rev. 40 (1995) 41.
[7] N.H. Goo, W.T. Jeong, K.S. Lee, J. Power Sources 87 (2000) 118.
[8] H.Y. Lee, N.H. Goo, W.T. Jeong, K.S. Lee, J. Alloys Comp. 2001 (in press).
[9] D.H. Ryan, F. Dumais, B. Patel, J. Kycia, J.O. Strom-Olsen, J. Less-Common Metals 172–174 (1991) 1296.
[10] K.S. Lee, C.J. Ha, Korean J. Mater. Res. 5 (1) (1995) 112.